Polym. Korea, Vol. 49, No. 1, pp. 148-157 (2025)
https://doi.org/10.7317/pk.2025.49.1.148
ISSN 2234-8077(Online)

# 탄소 양자점/폴리피롤/그래핀 산화물 기능화 폴리우레탄 폼 복합체의 슈퍼커패시터 결합 가스 센서 시스템

사마야난 셀밤 · 임진형†
공주대학교 공과대학 신소재공학부
(2024년 10월 7일 접수, 2024년 12월 17일 수정, 2024년 12월 17일 채택)

# Supercapacitor Combined Gas Sensor system from Carbon Quantum Dot/Polypyrrole/Graphene Oxide Functionalized Polyurethane Foam Matrixes

**Samayanan Selvam and Jin-Heong Yim†**
*Division of Advanced Materials Engineering, Kongju National University, Budaedong 275, Seobuk-gu, Cheonan-si, Chungnam 31080, Korea*
(Received October 7, 2024; Revised December 17, 2024; Accepted December 17, 2024)

**초록**: 폴리우레탄 폼(PUF)은 조절 가능한 기계적 및 신축성 특성으로 인해 폴리머 소재 이용 및 디바이스 설계에서 많은 연구가 이루어져 왔다. 본 연구에서는 PUF 매트릭스에 탄소 양자점(QD)과 폴리피롤(PPy) 및 그래핀 산화물(GO) 층의 형성을 통한 유연한 전기 전도성 PUF 복합체를 제조하였다. QD는 수열 합성 기술을 사용하여 바나나 껍질 고형 폐기물에서 합성되었다. 전도성 폴리머(CP)인 PPy는 PUF에 기상 중합 공정을 적용하고 GO와 QD의 함침 공정을 추가하여 PUF-PPy, PUF-PPy-QD, PUF-PPy-GO 복합체를 제조하고 슈퍼커패시터와 가스 센서 전극으로 적용하여 보았다. PUF-PPy-QD 및 PUF-PPy-GO 전극은 46 및 36 mF $cm^{-2}$의 면적 정전 용량을 각각 나타내었다. 또한 이러한 전극은 $NH_3$ 가스 감지 재료로 응용하였을 때, 우수한 감도와 반복성을 보여주었다. 본 연구 결과는 향후 활성 가스 센서와 슈퍼커패시터 시스템이 결합된 디바이스의 제조에 대한 간단하고 효과적인 경로를 제시할 수 있다.

**Abstract:** Polyurethane foam (PUF) is popular in polymer materials utilization and engineering due to their adjustable mechanical and stretchy assets. In this investigation, polypyrrole (PPy), carbon quantum dot (QD), and graphene oxide (GO) were used to produce flexible electro conductive PUF composites. The QD was synthesized from banana peel solid waste using hydrothermal technique. PPy as a conductive polymer (CP) was vapor-phased polymerized process on the PUF and formerly GO and QD were impregnated to produced PUF-PPy, PUF-PPy-QD, PUF-PPy-GO matrixes and examined for supercapacitor as well as gas sensor electrode. PUF-PPy-QD and PUF-PPy-GO electrodes revealed areal capacitances of 46 and 36 mF $cm^{-2}$. Also these electrodes have examined as an $NH_3$ gas sensing material and demonstrated fairly good sensitivity and repeatability. These findings highlight a simple and effective method for sustainable matrixes for the fabrication of active gas sensor combined supercapacitor system.

**Keywords:** sustainable ternary matrixes, polyurethane, polypyrrole, carbon quantum dot, gas sensor combined supercapacitor.

## Introduction

The demand for sustainable materials or matrixes for sensor combined energy storage units and reworking that are both economical and favorable to the environment are significantly increased, and smart devices that integrate for self-powered sensor and storage have attracted increasing attention as a major breakthrough for efficient usage. It is crucial and advantageous for wearable smart electronics devices to have an integrated energy storage system with multifunctional sensors.[1,2] Improving maintainable, versatile electrodes for use in smart energy storage and more specifically, in self-powered, multifunctional sensor device is currently a primary focus of sensor and energy storage research.[3]

Another important aspect is utilization of bio waste into sustainable materials, such as carbon quantum dot (QD). QD is a novel category of zero-dimensional carbon nanoparticles, predominantly composed of carbon and measuring less than 10 nm

†To whom correspondence should be addressed.
jhyim@kongju.ac.kr, ORCID 0000-0002-3557-9564

in size. They have garnered significant attention due to their extensive applications, including medical diagnosis, photo catalysis, fluorescent sensing and energy storage etc.[4] Consequently, significant efforts have been directed towards the advantageous synthesis of QD and the advancements of diverse applications. A variety of step-down procedures (laser ablation, electrochemical oxidation, and arc-discharge) and bottom-up approaches (microwave, ultrasonic, and hydrothermal techniques, etc.) have been discussed for the production of QD.[5-7]

There has been consistent development in gas sensor technology for the detection of explosives, pollutants, and toxic gases up to this point.[8,9] Many companies, including those dealing with chemicals, fertilizers, and food waste, produce ammonia through anaerobic digestion, which is one of the very dangerous gases. Ammonia gas can cause a host of health problems, including asthma, skin burns, serious respiratory irritation, and stable eye injury and blindness, even at low concentrations.[10,11] Next to the present time, a wide range of $NH_3$ gas sensors are accessible for purchase. The prior research indicates that numerous types of ammonia ($NH_3$) gas sensors are presently available on the market. Earlier research works indicate that the manufacturing of ammonia gas sensors has been explored using several techniques, including like, laser-based spectroscopy and crystal microbalances.[12-14]

Presently, a prevalent set of $NH_3$ gas sensor is which comprise an ionic and hydrogels. Nevertheless, due to the limited lifespan of this category of sensors and the low permanence of hydrogels throughout electrochemical processes, hybrid metals or ceramics combined with polymer matrixes or their products have been explored as substitutes.[15,16] Furthermore, several conductive polymer matrixes, carbon nanotubes, and reduced graphene oxide etc, have been demonstrated to be advantageous in chemistry and biosensors[17,18] owing to the simplicity of surface functionalized through uncomplicated chemical interactions.

Electrode materials for energy storage made of conductive polymer/metal composites or carbon based QD and GO have the potential to be stable over the long term, and sensor systems that combine cyclic stability with energy storage are essential for the creation of efficient smart electronic devices.[19,20] In general, custom-made electronic gadgets like smart bands, smart pens, and wearable health monitors can benefit from these kinds of sophisticated, self-powered, multifunctional sensor systems. Health monitoring and treatment are two areas where modern society is making great strides in the creation of smart electronic medical equipment.[21]

There has been a lot of recent focus on power source integrated sensor systems in the biosensor and energy storage research communities. Hygiene detection, bio-monitoring, and breathing analysis were the latest foci of Y. Su *et al*.'s self-powered respiration monitor system and conventional membrane sensor.[22,23] Wearable biosensors sensitive to Acetone, $NO_2$, and $NH_3$ were the primary targets of the energy transmission.[24,25] For smart electronics devices that may be worn, an integrated energy storage system with several functional sensors is crucial and advantageous. Smart energy storage, and more specifically self-powered multifunctional sensor device, is a current area of interest for sensor and energy storage researchers, who are working to develop better, more versatile electrodes.

We have previously reported caffeine, vanillin sensor integrated supercapacitor (SC) system,[26] also we have studied matrixes and various polymer composites for gas sensor system. To enhance conductivity, specific capacitance, mechanical stability, and flexibility, the integration of conducting polymers via GO and carbon quantum dot (QD) is advantageous and constitutes an effective approach. The PPy-GO composite is frequently utilized in the production of electrode materials because to PPy's superior conductivity, robust environmental stability, and straightforward synthesis. In our prior reports, we synthesized PUF-PPy for strain sensor applications and assessed the performance of PPy by the vapor phase polymerization (VPP) method.[27]

From the aforementioned observations and views, the present work focused its attention preceding the intention technique of gas sensor combined SC system, the progression assurance for structural constructions, fabrications route, and the electrical-mechanical comportment of PUF-PPy-GO and PUF-PPy-QD matrix as flexible gas sensor-SCs that were studied. The QD was prepared from banana peel waste. This is the first report on PUF and PPy combined bio waste derived QD matrix electrodes, and their performances have compared with GO combination matrixes.

## Experimental

**Details of Experiment Techniques. Chemicals Used:** The substrate used for the PUF-PPy fabrication process was PUF foundation (PMDI (Basf co., Lupranate M20R and PTMEG (BASF co. PEGTM 1800) used. Methanol and Ethanol (Samchun Pure Chemical) used as the solvent for the oxidizing mediator, iron(III) $\rho$-toluenesulfonate (FTS), during oxidative polymerization. The pyrrole (Py, ACROSE, GEEL, Belgium) monomer employed for oxidative polymerization of the conductive polymer PPy was utilized. The GO suspension 5 g/L purchased from Grapheneall (Lot.No.20200205).

**Bio Synthesis of QD From Banana Peel.** The bio derived QDs were produced after banana peel discarded using a straightforward hydrothermal technique.[28] The discarded waste was thoroughly pulverized with deionized water and subsequently put into an autoclave (Teflon liner). The autoclave was securely airtight and thereafter positioned in a household hot air oven, where it was passionate for 24 hours at 200 ℃. The resultant brownish-yellow simple product was carried out by filtration (membrane (0.22 μm).

The transparent brownish QD extracted liquid was separated, and the supernatant exhibited luminous characteristics. The acquired QD solution was refrigerated and preserved at 4 ℃ until utilized. To fulfill the requirements of characterizations, it was occasionally necessary to produce the sample as a solid, which was done as follows: A portion of the QD solution was extracted and subjected to vacuum freeze-drying for 4 hours to provide a solid brown powder QD. They were utilized for additional investigations.

**Production of PUF-PPy**: To fabricate PUF-PPy and, polyurethane (PU) was initially manufactured consuming 7 g of PMDI, Lupranate M20R, (i) NCO matrix = 30.0-32.0%, (ii) acid significance = max. 0.06 mg KOH/g, (iii) viscosity = 0.17–0.23 Pa·s) and 20 g of PTMEG.[29] The chamber temperature was maintained at 80 ℃ however swirling at 800 rpm for 60 sec. Subsequently, it was combined and agitated for 1 minute using distilled water, followed by a 10 min period to facilitate the generation of $CO_2$ gas, yielding soft PUF (Scheme 1(b)).

The PUF was submerged for 30 minutes in a 10 wt% solution of FTS, thereafter dried at ambient temperature for 12 hours, followed by oven drying at 60 ℃ for an extra 5 min. Subsequently, the PUF enclosing the oxidant (FTS) was transferred to a polymerization compartment.[30] Pyrrole was put next to the evaporation chamber for the VPP (Scheme 1(b); STEP I).

**Fabrication of PUF-PPy-GO and PUF-PPy-QD**: The cleaned PUF-PPy was engrossed in a GO solution (Grapheneall, 5 g/L) for 10 min to create the PUF-PPy-GO composites. The same procedure followed for PUF-PPy-QD. The prepared matrixes were subsequently dried at ambient temperature for 2 h and at 70 ℃ in a vacuum oven for 3 h. Then, these matrixes were rinsed with distilled water three times to eliminate deposits (Scheme 1(b); STEP II).

**Testing of QD and Matrix Analyzing Studies.** Transmission electron microscopy (TEM) (JEOL, JEM-2100) instrument, Fourier Transform Infrared spectrometer (FTIR, Perkin-Elmer), UV-Visible spectrum (UV), and photoluminescent (PL) employed for QD analysis. Micro-CT and Field Emission Scanning Electron Microscopy (FE-SEM) (TESCAN MIRA) were operated to analyze the morphology of the various composites. Hounsfield, H10KS-Universal Testing Machine (UTM) to check the mechanical strength studies. Electrochemical measurements

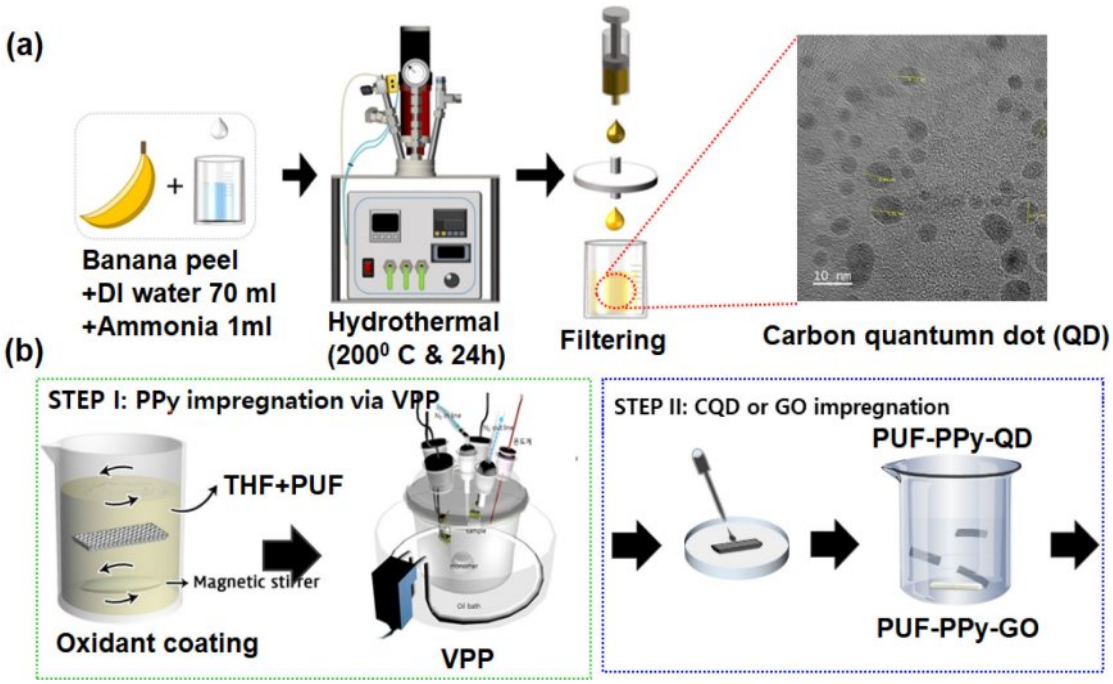


**Scheme 1.** (a) Preparation of QD from banana peel; (b) Fabrication process of various PUF based conductive composite.

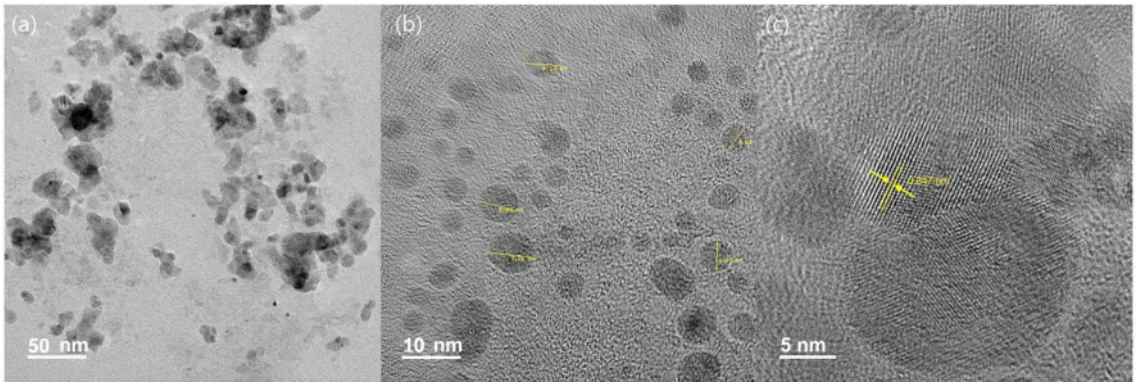


**Figure 1.** HRTEM images of prepared QD with various magnification.

of the SC's performance were taken exhausting a Workstation (SP-150, Biologic) and the gas sensor performance was tested by an inductor/capacitor/resistor (LCR) meter (GW Instek, LCR-6100).

## Results and Discussion

**TEM Studies of Bio Synthesized QD.** The QDs were produced from banana peel discarded using a straightforward hydrothermal method, as depicted in Figure 1(a-c). The morphology and dimensions of the produced QDs were analyzed using HRTEM. Figure 1(a) illustrates that the particle size collections from 5 to 7 nm, with a regular diameter of approximately 5 nm, indicating a broad dispersion and a spherical morphology. The HRTEM pictures (Figure 1(c)) indicate that the produced QDs possess distinct lattice fringes, suggesting a robust crystalline arrangement. The inside of QDs exhibits a significant degree of crystallinity in contrast to the outside surface, as evidenced by TEM images.[31]

**FTIR, UV-Visible and PL Studies Bio Synthesized QD.** The QDs were analyzed using FTIR spectroscopy. The bio synthesized QDs are thermally treated at 150, 200 and 230℃ temperature conditions thought to possess. The FTIR spectrum (Figure 2(a)) display peaks at approximately 3350 and 3250 $cm^{-1}$, attributed to the extending vibrations of -OH and N-H, correspondingly. C-H asymmetric and symmetric vibrations were detected at 2930 and 2850 $cm^{-1}$. The peaks at 1650, 1560, 1390, 1280, and 1070 $cm^{-1}$ resemble to the functional groups C-O, C-C, C-N-C, C-OH, and C-O-C, indicating the existence of $N_2$ and $O_2$ on the exterior of QDs.[32] The three temperature treatments showed not much difference in the functional groups shifts or modifications. These functionalities enhance the remarkable water solubility of QDs and indicate that the bio synthesized QDs will be advantageous for subsequent treatments and applications.

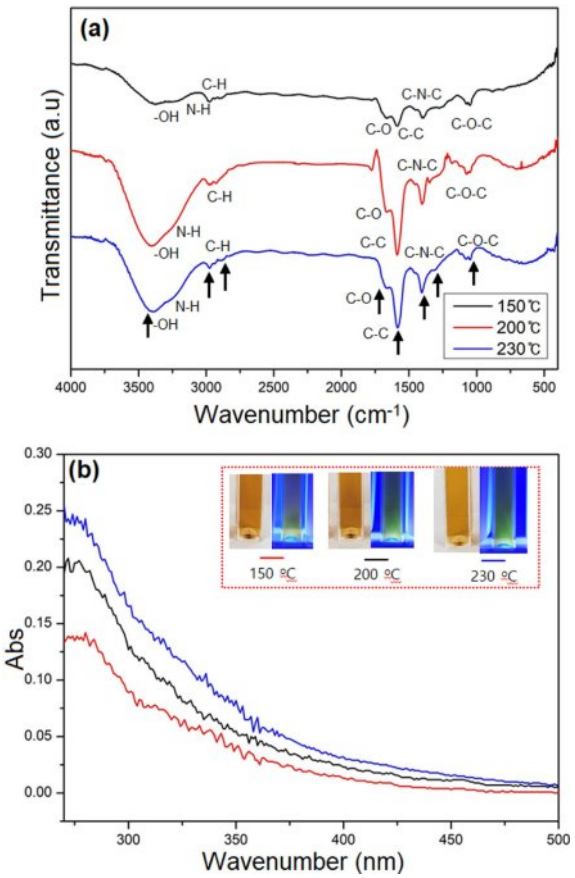


**Figure 2.** (a) FTIR spectra; (b) UV-Vis absorbance spectrum of prepared carbon QD with various synthesis temperature.

Figure 2(b) depicts the UV–Vis absorbance profile of the bio synthesized QDs after three temperature treatments (150, 200 and 230℃), which demonstrates the extensive absorption series at 270 and 320 nm in the UV region. These absorption

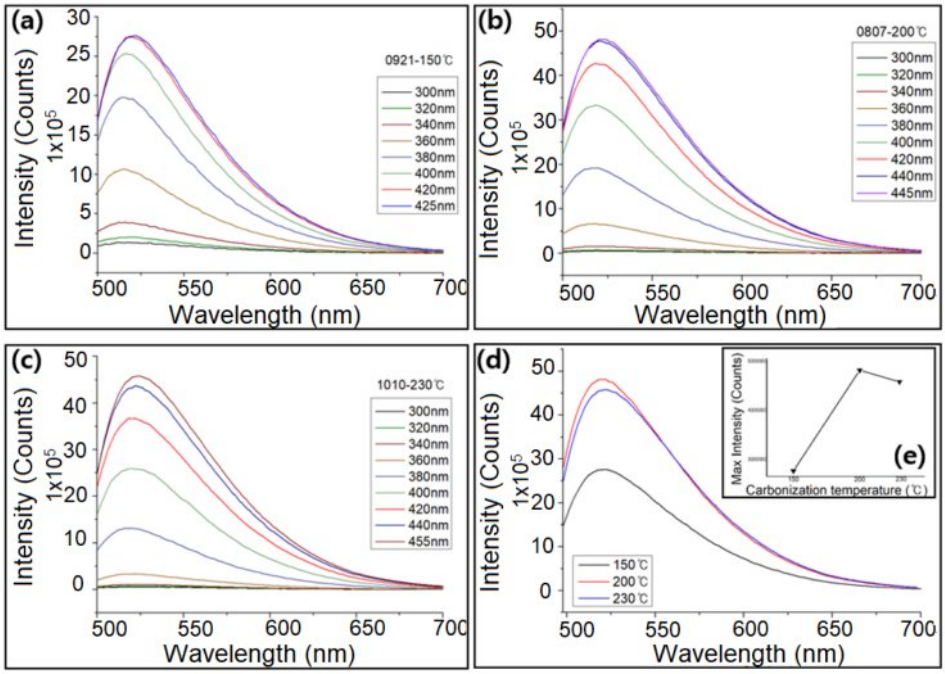


**Figure 3.** PL excitation spectra of biosynthesized QD with various temperatures.

ranges are associated to the distinctive π→π* transition band of the QD (C–C) sp2 hybrid orbitals and the n→π* transition band of the (C–O) sp3 hybrid orbitals, which are the efficient group on the exterior of QDs, correspondingly.[33] The insert optical images displayed the QDs under day light and UV light. According to the data presented in insert Figures, the final product of the bio synthesis of QDs is yellowish in aqueous solution when exposed to daylight, and it emits intense green fluorescence when excited by UV radiation.

The defining characteristic of QD is their PL activity, which is dependent on emission wavelength and size. From both necessary and applied perspectives, photoluminescence is one of the most intriguing properties of QDs. The produced carbon dots in aqueous solution exhibit green luminescence when exposed to UV light, as illustrated in the insert of Figure 2(b). The PL spectra of the carbon dots (Figure 3(a-c)) indicate that the PL intensity is depending upon the various temperature treated QD. The intensity of the photoluminescence spectra markedly upturns as the various conditions prepared QDs diminishes.[34] A significant presence of polar functionality facilitates agglomeration at elevated temperature treatments. The photoluminescence spectra of QD with varying excitation at 510 nm wavelength presented in Figure 3(d). A pronounced photoluminescence emission peaks were displaced to a longer wavelength with the elevation of the denoted wavelength, as evidently illustrated.

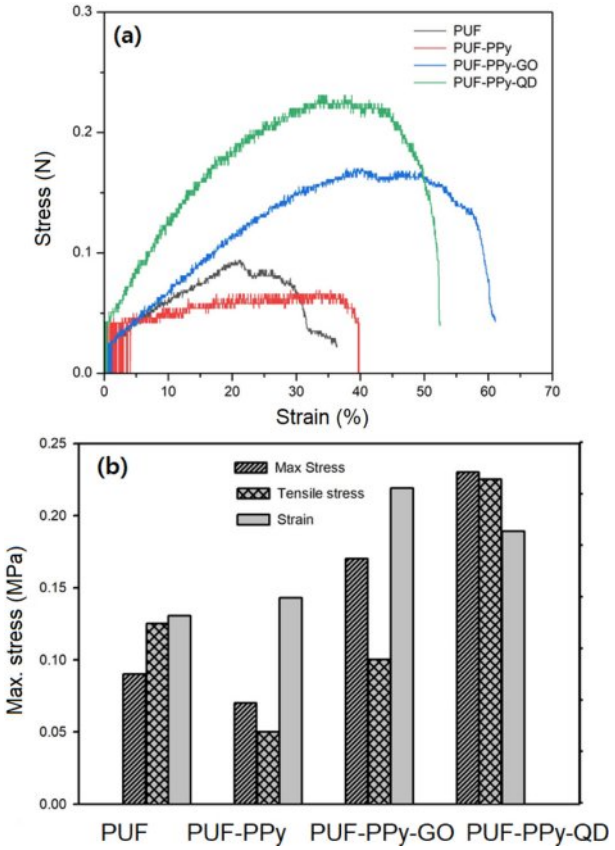


**Figure 4.** (a) Stress–strain curves for various PUF based composites; (b) Comparisons of mechanical properties of various PUF based composites.

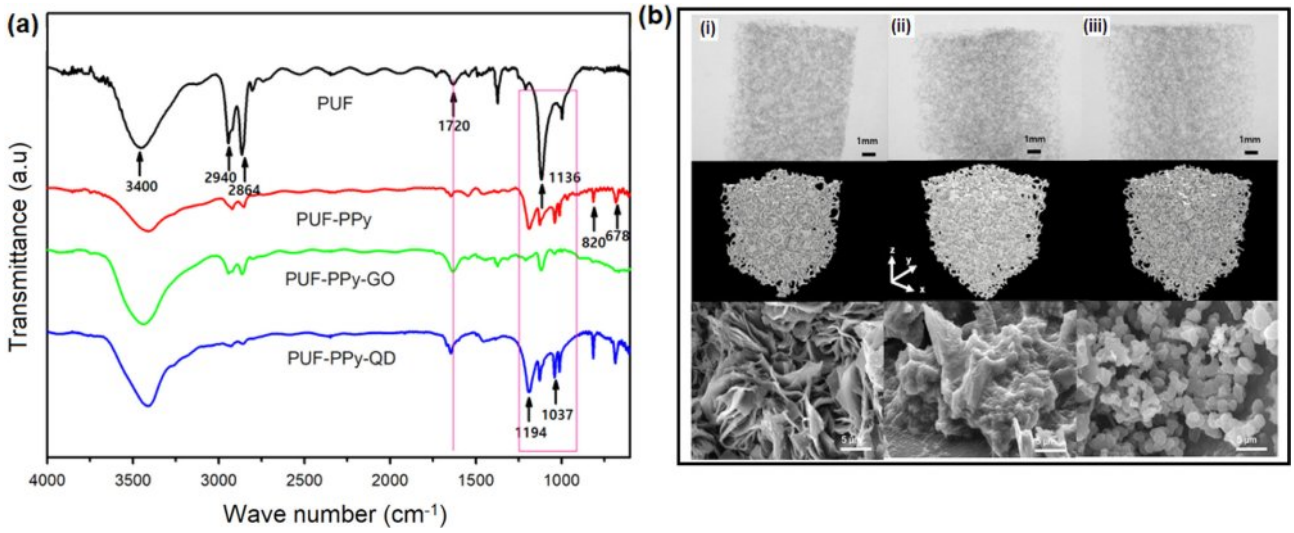


**Figure 5.** (a) FTIR spectra of prepared hydrophilic nitrogen-doped carbon QD with various synthesis temperatures; (b) micro-CT zoom-in images and SEM images of various PUF-based composite. (i) PUF-PPy, (ii) PUF-PPy-GO, (iii) PUF-PPy-QD, cross-sectional images (up panel) and 3D modeling images (middle panel) and surface SEM images with × 10,000 magnifications.

**Mechanical Strength and FTIR Studies of PPy, PUF-PPy/QD and PUF-PPy/GO Composites.** Figure 4 contrasts the mechanical belongings of PUF, PUF-PPy, QD and GO treated matrixes. The stress-strain curves and stress compressibility of PUF and PUF matrixes were assessed using UTM instrument.

The maximum tensile stress and strain can be determined from the stress-strain curves (Figure 4(a)) illustrated in Figure 4(b). Including conductive polymers like PPy into the PUF by vapor phase polymerization can slight decrease of mechanical properties, including maximum stress, and tensile stress due to the PPy's and depositions of GO or QD on the PUF-PPy composite, which resulted in improved mechanical characteristics. The PUF-PPy-QD and GO matrixes exhibited high maximum stress and tensile stress than PUF, respectively The maximum strain of the PUF-PPy-QD and PUF-PPy-GO were dramatically enhanced associated to PUF, demonstrating that QD and GO impregnation renders the PUF additional flexible and extensible due to more rigid secondary interactions between PUF and QD or GO.[31]

In imperative to study the chemical composition and interface between PUF, PUF-PPy, and PUF-PPy-QD and PUF-PPy-GO in matrixes FTIR analysis was carried out (Figure 5(a)). Various characteristic peaks were identified from polyurethane, such as 3400 $cm^{-1}$ (N-H stretching vibration peak), 2940 $cm^{-1}$ and 2864 $cm^{-1}$ (C-H), 1720 $cm^{-1}$ (C=O stretching) respectively.[35] After VPP, the FTIR results show that the N-H peaks that were previously attributable to PUF and PPy, which ranged in frequency from 3300 $cm^{-1}$, widened significantly because PPy was present. In PPy, the peak at 1042 $cm^{-1}$ is the C-H bending peak, and the two peaks appearing at 820 and 678 $cm^{-1}$ are due to the C-H out-of-plane warp stretching peaks of pyrrole ring,[36] indicating the successful polymerization of PPy. The peaks, located at 1194, and 1037 $cm^{-1}$, are related to the functional groups C-N-C, C-OH.[37]

**Morphological Analysis of PPy-GO and PUF-PPy-QD Composites.** The porous constructions and distribution of PUF and different PUF-PPy matrixes like PUF-PPy-GO, and PUF-PPy-QD were studied using micro-CT and SEM pictures, which can be seen in Figure 5(b(i-iii)). Micro pores in PUF-PPy, PUF-PPy-GO and PUF-PPy-QD are open networks of constructions that are connected to each other. Interestingly, unevenly curved surfaces were seen on the pure PUF-PPy (bottom picture of the Figure 5(b(i)). The rough areas of PUF, on the other hand, became smooth after being impregnated with GO and QD.

The SEM images clearly displayed, the GO sheets and QDs look like they cover and swallow up all of the PUF's sides. Since the surface of GO sheets and QD is smooth and uniform. As demonstrated in the SEM of PUF-PPy and PUF-PPy-GO and PUF-PPy-QD, the combined morphology changed from thin layers blocks to aggregated GO sheets and QD granular appearances.

**Electrochemical Characterizations of PUF-PPy and PUF-PPy-QD and PUF-PPy-GO constructed SCs.** The Figure

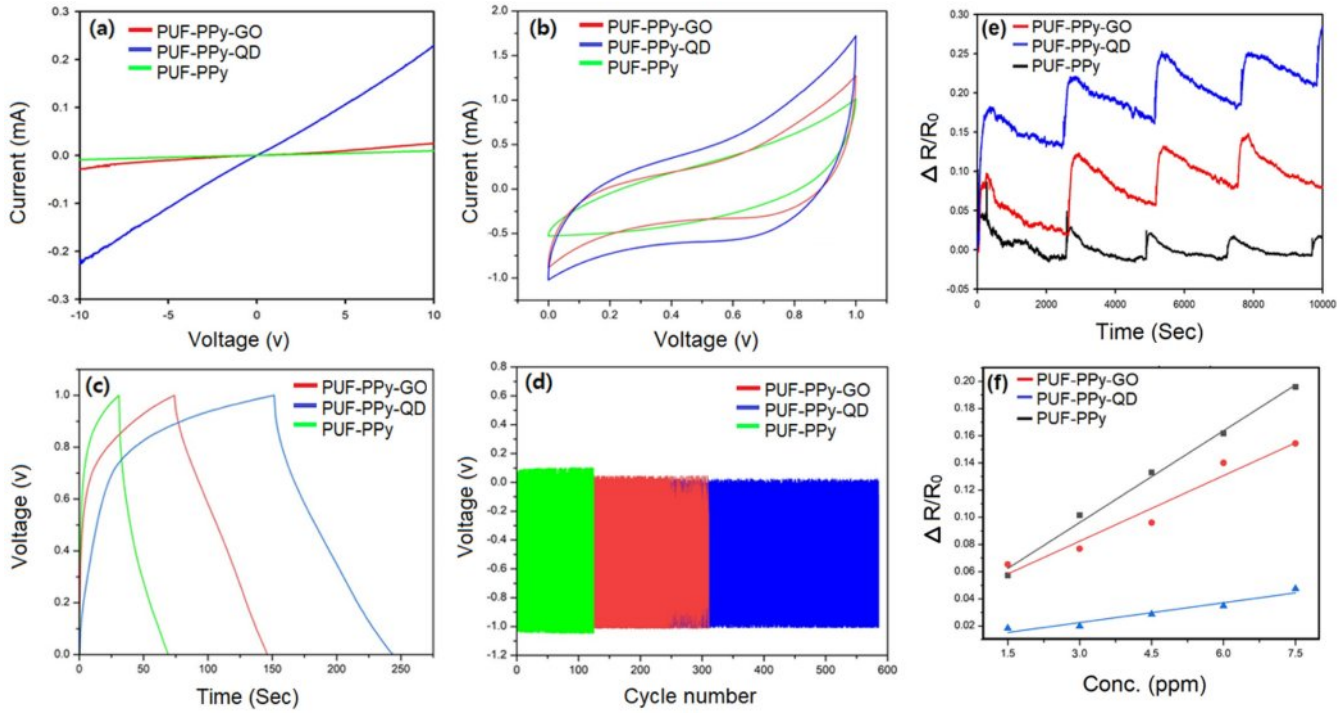


**Figure 6.** Electrochemical analysis of various PUF based composites: (a) I−V curve; (b) CV curve; (c) galvanostatic charge−discharge profile; (d) stability for various PUF composites prepared with different fabrication processes; (e) behaviors of gas sensors for repeatability of detection response of different PUF composites at 7.5 ppm; (f) sensitivity as a function of ammonia concentration.

6(a) shows the I-V profile for PUF-PPy, PUF-PPy-QD and PUF-PPy-GO. The graph show that the porous compounds that were made behave normally in terms of ohmic reactions. PUF-PPy-QD exhibits much higher current value than PUF-PPy-GO, which suggests that it conducts electricity better. PUF-PPy-QD used on the SC and gas sensor device. The electrochemical performances of the PUF-PPy and PUF-PPy-QD and PUF-PPy-GO SC electrodes inspected from a workstation (SP-150, BioLogic). This instrument was working to attain the consistent cyclic voltammetry (CV), and galvanostatic charge-discharge (CD). The SC electrode was made using a symmetric sandwich-type structure. The sandwich-type system was used to make the composite film SC. For more details, an electrolyte made of 6 M KOH as created for use in SC electrodes. As well, filter paper (Whatman) was used as separator. Figure 6(b) shows the CV images of the PUF-PPy, PUF-PPy-QD, and PUF-PPy-GO-based SCs that were gathered at 25 mV/s scan speed. The CV characteristics of QD and GO decorated electrodes were typical symmetrical and exhibited two distinct sets of redox peaks, signifying that the material's nature was pseudocapacitive. The PUF-PPy-QD and PUF-PPy-GO supercapacitors have an enlarged region of the cyclic voltammetry curve in comparison to PUF-PPy. The normal redox peaks were found to be consistent.[38]

Figure 6(c) illustrates the GCD data with current density of 0.25 mA. The obtained GCD curve exhibited a tendency analogous to the triangular and reasonably symmetrical shapes of the PUF-PPy, PUF-PPy-QD, and PUF-PPy-GO curves. Furthermore, the charging and discharging intervals were standard. The GCD profiles of all composite SCs display their characteristic curves. This clearly confirms the pseudo-capacitance and electric double-layer capacitor characteristics of the PUF-PPy-QD and PUF-PPy-GO electrode materials. Furthermore, the curves are linear and symmetrical. A negligible amount of the standard internal resistance was observed in every discharge curve. Through the employment of quick surface adsorption-desorption reactions, electrode materials with high electrical conductivity can enhance electron charge transfer reactions at the interface. The galvanostatic discharge curves were used to determine the specific capacitance, and equation (1) was applied to assess the performance.[39]

$$C = \frac{I\Delta t}{A\Delta V} \tag{1}$$

**Table 1. Comparisons of Electrochemical Properties and Ammonia Sensor Performances of Various PUF Based Composites Prepared with Different Fabrication Processes**

| Samples | Resistance ($\Omega$ cm$^{-2}$) | Electrical conductivity (S cm$^{-2}$) | Capacitance (mF cm$^{-2}$) | $NH_3$ sensing gauge factor ($\Delta R/R_o$*100) | Coefficient of determination ($R^2$) |
|---|---|---|---|---|---|
| PUF-PPy | $3.96 \times 10^8$ | $2.525 \times 10^{-7}$ | 19.08 | 0.93 | 0.92 |
| PUF-PPy-GO | $4.99 \times 10^5$ | $2.001 \times 10^{-6}$ | 36.08 | 7.28 | 0.94 |
| PUF-PPy-QD | $2.74 \times 10^5$ | $3.655 \times 10^{-6}$ | 46.10 | 9.43 | 0.99 |

The abbreviations $I$(A) denote current, $t$(s) signifies the duration time for complete discharge, $A$(cm$^2$) denotes the area of electrode, and V indicates the voltage change following full charge or discharge. The acquired areal capacitances are illustrated in Table 1. The specific capacitances of the composite electrodes have been evaluated using the discharge curves. The specific capacitance of the PUF-PPy, PUF-PPy-QD, and PUF-PPy-GO composite supercapacitors were 19.08, 46.1, and 36.08 mF cm$^{-2}$, respectively. This is a substantial enhancement compared to the PUF-PPy-QD and PUF-PPy-GO SC, demonstrating the influence on the polymerization process and QD. GO coatings exhibit excellent performance and significant enhancements following QD and GO treatments.

The Figure 6(d) indicates that cyclic stability is an additional factor for assessing the performance of the supercapacitor. The composite supercapacitors composed of PUF-PPy, PUF-PPy-QD, and PUF-PPy-GO were examined for their long-term cyclic stability over 500 cycles by GCD testing. The capacitive properties of QD/GO-coated supercapacitors can be enhanced, as the loading of QD/GO may result in considerable agglomeration and restacking of PPy and QD.[38] The electrochemically active mass transport network of PPy and QD, facilitating electron transfer between the two materials and significantly contributing to the capacitance of PPy. Moreover, the composite-based supercapacitor device exhibited superior capacitance and cycling stability attributable to the PPy and QD/GO tight bonds with the PUF sheets.

**$NH_3$ Gas Sensor Evaluation of the PUF–PPy-QD and PUF–PPy-GO**. Figure 6(e, f). Illustrate the usual resistance variations for assessing the $NH_3$ gas sensing efficacy of PUF-PPy-QD and PUF-PPy-GO at 7.5 ppm of $NH_3$ over time. The PUF-PPy-QD demonstrates efficient detection capability after many injections of $NH_3$ (Figure 6(e)). The detection efficacy of PUF-PPy, PUF-PPy-QD, and PUF-PPy-GO was examined. PUF-PPy exhibited significant signal noise, resulting in inconsistent $NH_3$ detection concert. The PUF-PPy exhibited distinct signals; nevertheless, it lacked steadiness in the bounty of resistance variations. The incorporation of QD and GO into the PUF-PPy enhances the $NH_3$ detection signals.

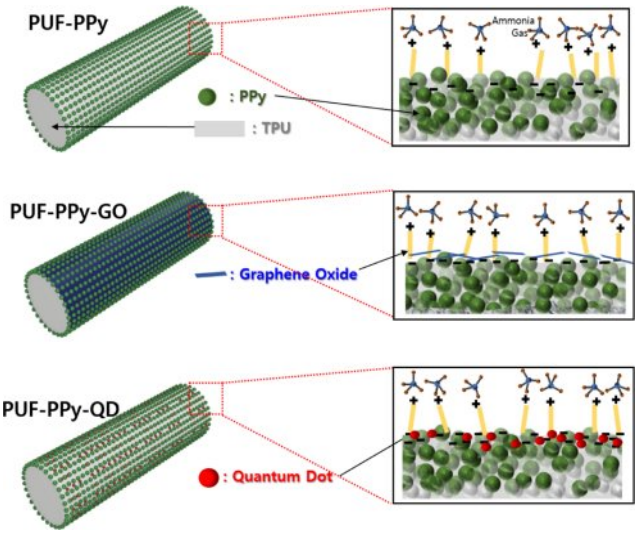


**Figure 7.** Illustration of how these three different materials interact with ammonia molecules.

We concentrate on PUF-PPy-QD for the detection of ammonia. The rise in electrical resistance associated with the reduction in current in the PPy-based matrixes is attributable to the electron-donating properties of $NH_3$. Prior research demonstrated a comparable occurrence of current reduction following exposure to $NH_3$ gas, attributed to the nitrogen's lone pair of electrons, which can readily be transferred to the first oxidized PPy.[40,41]

The lone electron pairs neutralize the positively charged PPy's ions, leading to a reduction in the number of carriers, which consequently decreases current and increases electrical resistance, as demonstrated in this instance. The sensor's reaction to low concentrations of $NH_3$ was additional examined and demonstrated strong linearity, with a coefficient of $d > 0.90$ (Figure 6(f). The sensor performance of bio-synthesized QD mediated composite is higher than GO coated composites.

Figure 7 elucidates the gas detecting principle of the constructed electrode. The intricate architecture of PPy, QD and GO

facilitates the adsorption of ammonia gas molecules. The conductivity related to carrier concentration of the PPy main chain was influenced by the "electronic sensitization" between QD and GO and $NH_3$ gas molecules.

The $NH_3$ detection by the constructed electrode occurs by an external-controlled mechanism involving electron transfer between the gas and the electrode. When gas is introduced to the electrode, the gas molecules are adsorbed onto the QD and GO coated composite. The gas molecules adsorbed are oxidized by electrons in the PPy main chain, resulting in an increase in the electrode's resistance due to electron loss. The oxidized $NH_3$ gas molecules can be readily desorbed from the electrode surface. Moreover, the bio synthesized QD and GO as an electrical stimulation of the materials on PUF-PPy surfaces have been shown to exhibit comparable patterns, as indicated by pervious reports. [42, 43] This stimulation results in the injection of electrical charge into the electrode layers, which in turn promotes interactions between the composite layers.

## Conclusions

We have successfully synthesized QD from food waste banana feel via hydrothermal technique. The bio-synthesized QD also incorporated with PUF-PPy matrix for enhanced electrical conductivity and mechanical stability. These performances compared with GO coating. The PUF-PPy-QD and PUF-PPy-QD electrodes fabricated as supercapacitor combined gas sensor system. PUF-PPy-QD and PUF-PPy-GO electrodes have 46 and 36 $mFcm^{-2}$ areal capacitances. These electrodes also tested as $NH_3$ gas sensing materials and showed high sensitivity. Specifically, PUF-PPy-QD demonstrated good sensitivity as well as repeatability for $NH_3$ gas detection. This study suggests that composites may be suitable for sensor combined supercapacitor system for the future smart device applications.

Acknowledgments. This research was supported by the Basic Science Research Program through a National Research Foundation of Korea (NRF) grant funded by the Korean government (MSIT) (No. RS-2023-00221237). This work was also supported by the National Research Foundation of Korea (NRF) grant funded by the Korea government (MSIT) (No. RS-2024-00335799). Also, this work was supported by the research grant of Kongju National University in 2024.

Conflict of Interest: The authors state that there is not at all conflict of interest.

## References

1. Zhang, J.; Gu, M.; Chen, X. Supercapacitors for Renewable Energy Applications: A Review. *Micro Nano Eng*. **2023**, 21, 100229.
2. Ma, T.; Yang, H. X.; Lu, L. Development of Hybrid Battery-supercapacitor Energy Storage for Remote Area Renewable Energy Systems. *Appl. Energy* **2015**, 153, 56-62.
3. Amir, M.; Deshmukh, G. R.; Khalid, M. H.; Said, Z.; Raza, A.; Muyeen, S. M.; Nizami, A.; Elavarasan, R. M.; Saidur, R.; Sopian, K. Energy Storage Technologies: An Integrated Survey of Developments, Global Economical/environmental Effects, Optimal Scheduling Model, And Sustainable Adaption Policies. *J. Energy Storage* **2023**, 72, 108694.
4. Sharma, S.; Kumar, R.; Kumar, K.; Thakur, N. Sustainable Applications of Biowaste-derived Carbon Dots in Eco-friendly Technological Advancements: A Review. *Mater. Sci. Eng. B* **2024**, 305, 117414.
5. Nazar, M.; Hasan, M.; Basuki, W.; Gani, B. A.; Nada, C. E. Microwave Synthesis of Carbon Quantum Dots from Arabica Coffee Ground for Fluorescence Detection of $Fe^{3+}$, $Pb^{2+}$, and $Cr^{3+}$. *ACS Omega* **2024**, 9, 20571-20581.
6. Qi, C.; Wang, H.; Yang, A.; Wang, X.; Xu, J. Facile Fabrication of Highly Fluorescent N-Doped Carbon Quantum Dots Using an Ultrasonic-Assisted Hydrothermal Method: Optical Properties and Cell Imaging. *ACS Omega* **2021**, 6, 32904-32916.
7. Pontes, S. M. A.; Rodrigues, V. S. F. One-pot Solvothermal Synthesis of Full-color Carbon Quantum Dots for Application in Light Emitting Diodes. *Nano-Struct. Nano-Objects* **2022**, 32, 100917.
8. Güntner, A. T.; Righettoni, M.; Pratsinis, S. E. Selective Sensing of $NH_3$ by Si-doped α-$MoO_3$ for Breath Analysis. *Sensor. Actuat. B-Chem*. **2016**, 223, 266-273.
9. Hibbard, T.; Crowley, K. Point of Care Monitoring of Hemodialysis Patients with a Breath Ammonia Measurement Device Based on Printed Polyaniline Nanoparticle Sensors. *Anal. Chem*. **2013**, 85, 12158-12165.
10. Ji, X.; Banks, C. E.; Aldous, L. Electrochemical Ammonia Gas Sensing in Nonaqueous Systems: a Comparison of Propylene Carbonate with Room Temperature Ionic Liquids. *Electroanalysis* **2007**, 19, 2194-220.
11. Oudenhoven, J. F. M.; Knoben, W. Electrochemical Detection of Ammonia Using a Thin Ionic Liquid Film as the Electrolyte. *Procedia Eng*. **2015**, 120, 983-986.
12. Quy, N. V.; Minh, V. A. Gas Sensing Properties at Room Temperature of a Quartz Crystal Microbalance Coated with ZnO Nanorods. *Sensor. Actuat. B-Chem*. **2011**, 153, 188-193.
13. Kwak, D.; Lei, Y.; Maric, R. Ammonia Gas Sensors: A Comprehensive Review. *Talanta* **2019**, 201, 713-730.
14. Ahmad, H. A.; Rizky, A. Ultra-sensitive Ammonia Sensor Based on a Quartz Crystal Microbalance Using Nanofibers Overlaid with Carboxylic Group-functionalized MWCNTs. *Analyst*, **2024**, 149, 5191-5205.
15. Chokkareddy, R.; Niranjan, T.; Redhi, G. G. Chapter 13 - Ionic

Liquid Based Electrochemical Sensors and Their Applications. In *Green Sustainable Process for Chemical and Environmental Engineering and Science*; Inamuddin; Asiris, A. M.; Karchi, S., Eds.; Elsevier: Amsterdam, Cambridge, 2020; pp 367-387.
16. Hussain, S.; Maktedar, S. S. Structural, Functional and Mechanical Performance of Advanced Graphene-based Composite Hydrogels. *Results Chem.* **2023**, 6, 101029.
17. Jurgis, B.; Lina, M. Single-walled Carbon Nanotube Based Coating Modified with Reduced Graphene Oxide for the Design of Amperometric Biosensors. *Mater. Sci. Eng. C* **2019**, 98, 515-523.
18. Hussain, M. F.; Slaughter, G. PtNPs Decorated Chemically Derived Graphene and Carbon Nanotubes for Sensitive and Selective Glucose Biosensing. *J. Electroanal. Chem.* **2020**, 861, 113990.
19. Shao, C.; Zhao, Y.; Qu, L. Recent Advances in Highly Integrated Energy Conversion and Storage System. *SusMat.* **2022**, 2, 142-160.
20. Mousavi, M. S.; Hashemi, A. S.; Kalashgrni, M. Y. Recent Advances in Energy Storage with Graphene Oxide for SC Technology. Sustainable *Energy Fuels* **2023**, 7, 5176-5197.
21. Marzo, G.; Mastronadri. V. M. Sustainable Electronic Biomaterials for Body-compliant Devices: Challenges and Perspectives for Wearable Bio-mechanical Sensors and Body Energy Harvesters. *Nano Energy* **2024**, 123, 109336.
22. Wang, S.; Jiang. Y. An Integrated Flexible Self-powered Wearable Respiration Sensor. *Nano Energy* **2019**, 63, 103829.
23. Dai, J.; Li, L.; Shi, B.; Li, Z. Recent Progress of Self-powered Respiration Monitoring Systems. *Biosens. Bioelectron.* **2021**, 194, 113609.
24. Hong, H. S.; Ha, N. H. Enhanced Sensitivity of Self-powered $NO_2$ Gas Sensor to Sub-ppb Level Using Triboelectric Effect Based on Surface-modified PDMS and 3D-graphene/CNT Network. *Nano Energy* **2021**, 87, 106165.
25. Kolmakov, A.; Klenov, D. O,; Lilach, Y. Enhanced Gas Sensing by Individual $SnO_2$ Nanowires and Nanobelts Functionalized with Pd Catalyst Particles. *Nano Lett.* **2005**, 5, 667-673.
26. Selvam, S.; Yim, J.-H. Multifunctional Supercapacitor Integrated Sensor from Oyster and Cicada Derived Bio-ternary Composite: Vanillin/caffeine Detections in Beverages. *J. Energy Storage* **2022**, 45, 103791.
27. Jo, Y. H.; Selvam, S.; Yim, J.-H. Assembly of Flexible 3D Printed SCs from Thermoplastic Polyurethane Embedded Polypyrrole-CuO/$MnO_2$ Composites. *Polym. Korea* **2024**, 48, 289-298.
28. Han, L.; Guo, T. Preparation of Carbon Quantum Dot Fluorescent Probe from Waste Fruit Peel and Its Use for the Detection of Dopamine. *RSC Adv.* **2024**, 14, 1813-1821.
29. Park, J. S.; Yim, J.-H. Mechanically and Electrically Enhanced Polyurethane-poly(3,4-ethylenedioxythiophene) Conductive Foams with Aligned Pore Structures Promote MC3T3-E1 Cell Growth and Proliferation. *ACS Appl. Polym. Mater*. **2020**, 1482-1490.
30. Kim, Y. J.; Yim, J.-H. Flexible, Biocompatible, and Electroconductive Polyurethane Foam Composites Coated with Graphene Oxide for Ammonia Detection. *Sensor. Actuat. B-Chen.* **2021**, 344, 130269.
31. De, B.; Karak, N. A Green and Facile Approach for the Synthesis of Water Soluble Fluorescent Carbon Dots From Banana Juice. *RSC Adv.* **2013**,3, 8286-8290.
32. Atchudan, R.; Edison, T. N. J. I. D. Facile Green Synthesis of Nitrogen-doped Carbon Dots Using Chionanthus Retusus Fruit Extract and Investigation of Their Suitability for Metal Ion Sensing and Biological Applications. *Sensor. Actuator. B-Chen.* **2017**, 246, 497-509.
33. Brachi, P. Synthesis of Carbon Dots (CDs) Through the Fluidized Bed Thermal Treatment of Residual Biomass Assisted by $\gamma$-alumina. *Appl. Catal. B Environ*. **2020**, 263, 118361.
34. Kalaiyarasan, G.; Hemlatha, C.; Joseph, J. Fluorescence Turn-On, Specific Detection of Cystine in Human Blood Plasma and Urine Samples by Nitrogen-Doped Carbon Quantum Dots. *ACS Omega* **2019**, 4, 1007-1014.
35. Hatchett, D. W.; Kodippil, D. FTIR Analysis of Thermally Processed PU Foam. *Polym. Degrad. Stab.* **2005**, 87, 555-561.
36. Cho, H.-J.; Noh, Y.-J.; Jin, E-Y.; Yim J.-H. Study on the Hybrid Dual-functioning Application of Urethane Foam Modified with Graphene Oxide and Polypyrrole for an Electrode Scaffoldas Well as Chemical Sensor. *Polym. Korea* **2023**, 47, 453-462.
37. Bertolini, C. M.; Zamperlin, N.; Barra, G. M. O.; Pegoretti, A. Development of Poly(vinylidene fluoride)/thermoplastic Polyurethane/carbon Black-polypyrrole Composites with Enhanced Piezoelectric Properties. *SPE Polymers* **2023**, 4, 143-155.
38. Malik, R.; Lata, S.; Soni, Y.; Rani, P.; Malik, R. S. Carbon Quantum Dots Intercalated in Polypyrrole (PPy) Thin Electrodes for Accelerated Energy Storage. *Electrochim. Acta* **2024**, 364, 137281.
39. Selvam, S.; Park, Y-K.; Yim, J.-H. An Extremely Low Temperature Environment Operatable Hybrid Dual-functioning Energy Device Driven by a Supercapacitor/piezo–triboelectric Generator System. *J. Mater. Chem. A* **2023**, 11, 16973-16984
40. Fernandez, F. D. M.; Khadka, R.; Yim, J.-H. Highly Porous, Soft, and Flexible Vaporphase Polymerized Polypyrrole–styrene–ethylene–butylene–styrene Hybrid Scaffold as Ammonia and Strain Sensor. *RSC Adv.* **2020**, 10, 22533-22541.
41. Bhat, N. V.; Gadre, A. P. Bambole, V. A. Structural, Mechanical, and Electrical Properties of Electropolymerized Polypyrrole Composite Films. *J. Appl. Polym. Sci*. **2001**, 80 2511-2517.
42. Choi, K. S.; Liu, F. Fabrication of Free-standing Multilayered Graphene and Poly(3,4-ethylenedioxythiophene) Composite Films with Enhanced Conductive and Mechanical Properties. *Langmuir* **2010**, 26, 12902-12908.
43. Zhai, Y.; Yu, Y. Flexible and Wearable Carbon Black/thermoplastic Polyurethane Foam with a Pinnate-veined Aligned Porous Structure for Multifunctional Piezoresistive Sensors. *Chem. Eng. J.* **2020**, 382, 122985.